JOURNAL OF CATALYSIS 96, 170–181 (1985)

Redispersion of Pt–Ir Supported on γ-Al_2O_3 and SiO_2 in Chlorine-Containing Gases

K. FOGER, D. HAY, AND H. JAEGER

CSIRO Division of Materials Science, Locked Bag 33, Clayton 3168 Australia

Received January 16, 1985; revised May 12, 1985

Model catalysts consisting of bimetallic Pt–Ir or separate Pt and Ir particles supported on γ-Al_2O_3 and on SiO_2 have been reacted in a flow system at atmospheric pressure with Cl_2 in N_2 or Cl_2 mixed with NO or CO in N_2 at selected temperatures in the range 570–670 K. The catalysts were examined using X-ray diffraction (XRD), transmission electron microscopy (TEM), and temperature-programmed reduction (TPR). Bimetallic Pt–Ir particles supported on Al_2O_3 could be successfully redispersed in Cl_2/N_2 streams at temperatures in the range 570–670 K. Redispersion occurred via a mixed chloride of Pt and Ir which is either an adduct similar to $PtAl_2Cl_8$ or a hexameric Pt_6Cl_{12} molecule with some Ir atoms exchanged for Pt. In mixtures of Pt and Ir particles on γ-Al_2O_3 only Pt was redispersed, but Ir remained agglomerated. Extensive metal losses were found to occur with CO and Cl_2 in the treatment gas. However, NO mixed with Cl_2 proved suitable for the redispersion of both Pt and Ir. The formed small metal particles are most likely bimetallic. In SiO_2-supported catalysts treatment with either Cl_2, Cl_2 + CO, or Cl_2 + NO could not achieve redispersion.

INTRODUCTION

Bimetallic Pt–Ir particles supported on γ-Al_2O_3 exhibit a higher selectivity and lower tendency to coke formation than either Pt or Pt–Re reforming catalysts (*1*). However, the regeneration of Pt–Ir catalysts proves to be a difficult task. Under conditions generally used to remove coke and poisons from the catalysts (oxidizing atmospheres, $T > 700$ K), iridium forms volatile oxides which precipitate as large crystals, separate from the alloy particles (*2*). Simply redispersing the iridium is not sufficient for regeneration, since only bimetallic Pt–Ir possesses the desired reforming features (*1*). Treatments with halogen-containing gases at $T > 600$ K are commonly employed to redisperse agglomerated metals in supported-metal catalysts (*3*), and recently redispersion procedures particularly suited for catalysts containing iridium have been reported (*14*). Detailed studies on the redispersion of platinum (*4*) and iridium (*5*) on γ-alumina in chlorine-containing atmospheres have shown that platinum is readily redispersed, but for iridium additions of volatilization agents (such as CO and NO) are essential.

In this study catalysts containing either Pt–Ir alloy particles or mixtures of Pt and Ir particles on SiO_2 and γ-Al_2O_3 were exposed to chlorine-containing atmospheres in the temperature range 570–700 K and subsequently examined using X-ray diffraction (XRD), transmission electron microscopy (TEM), and temperature-programmed reduction (TPR).

EXPERIMENTAL

The following catalysts were studied:

Catalyst A, 2.0% Pt–Ir (ratio 1.0) on γ-Al_2O_3. The support (Merck, 125 $m^2\ g^{-1}$) was impregnated with H_2PtCl_6 and H_2IrCl_6 in H_2O and air-dried at 370 K. TPR was carried out on 0.1 g of sample (Fig. 8, trace: —). The bulk of the sample was reduced in flowing H_2 (6 liters hr^{-1}) at 670 K for 15 hr. The metal was present as small particles ($\bar{d} < 2$ nm) distributed evenly over the support (Fig. 1a). The composition could not be determined with XRD or TEM, but EXAFS data (*6*) yielded a metal–metal nearest-neighbor distance of 0.2740 nm

0021-9517/85 $3.00

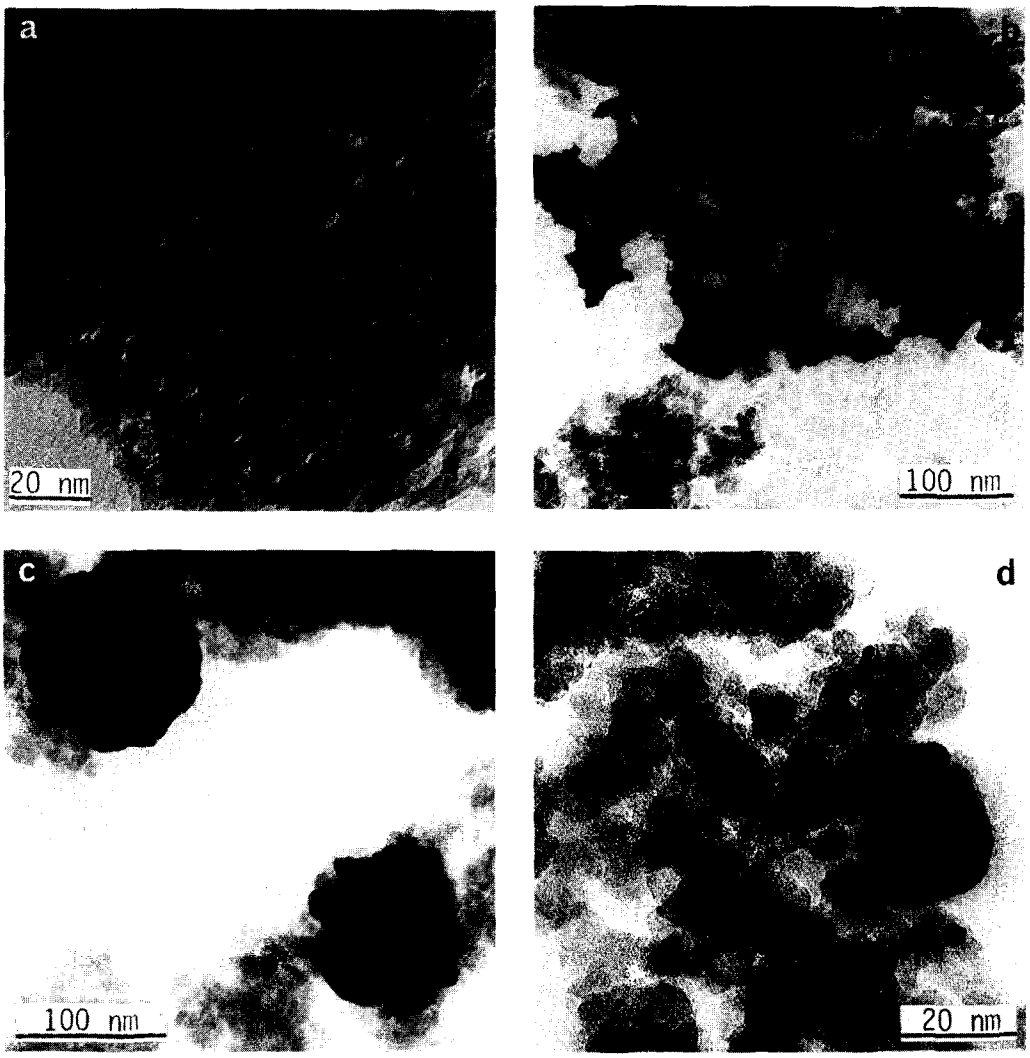

FIG. 1. Electron micrographs showing metal particles in Catalysts (a) A, (b) B, (c) C, and (d) D.

compared to 0.2775 for Pt and 0.2714 for Ir. This indicates that the particles are bimetallic, in agreement with results of Sinfelt *et al.* (7).

Catalyst A1 was prepared by treating catalyst A in 1% O_2/He at 820 K for 5 hr followed by reduction in flowing H_2 at 670 K for 15 hr. This catalyst consisted of small ($\bar{d} < 3$ nm) platinum particles and large ($\bar{d} > 10$ nm) needlelike iridium agglomerates (2).

Catalyst B, 2.15% Pt–Ir (ratio 0.9) on γ-Al_2O_3. The γ-Al_2O_3 support (Merck, 125 m^2 g^{-1}) was mixed with $PtCl_2$ and $IrCl_3$ in a ball mill. 0.1 g of sample was reduced by TPR (Fig. 9, trace: ---). The rest of the sample was treated with flowing H_2 (6 liters hr^{-1}, 670 K, 15 hr). Metal particles of this catalyst are shown in Fig. 1b. They consisted of large agglomerates of both Pt and Ir, and the XRD profile (Fig. 6) shows two clearly separated metal 111 peaks. The mean crystallite size estimated from their half-widths is larger than 20 nm for both metals.

Catalyst C, 3.6% Pt–Ir (ratio 1.22) on γ-Al_2O_3. Alumina (Merck, 125 m^2 g^{-1}) was stirred in a solution containing hydrazine hydrochloride and ammonia (pH 9) at 350

K, and a dilute solution of H_2PtCl_6 and H_2IrCl_6 was added dropwise. The slurry was stirred for 2 hr at 350 K, filtered, and air-dried at 370 K. The catalyst was then reduced in flowing H_2 at 670 K for 15 hr. The metal particles, Fig. 1c, were spherical agglomerates of crystallites, d = 100 nm. The mean crystallite size determined from XRD was 10–20 nm. The XRD peak profile (Fig. 3) is symmetric, and the 2θ value at maximum intensity is between that expected for pure Pt and that for pure Ir. From the peak shape and position it is assumed that the metal was in the form of a platinum–iridium alloy.

Catalyst D, 8.9% Pt–Ir (ratio 1.0) on SiO_2. The catalyst was prepared by impregnating Aerosil 200 (Degussa) to incipient wetness with H_2PtCl_6 and H_2IrCl_6 in H_2O, drying it in air, and then exposing it to flowing H_2 at 670 K for 15 hr. The metal particles were within a size range 2–40 nm (Fig. 1d). The XRD trace (Fig. 1l) shows a symmetric metal 111 peak halfway between the Pt and Ir peak positions. This supports the premise of predominantly bimetallic particles in the catalyst.

Catalyst samples (0.5–1.0 g) were placed in a vertical fused-silica reactor tube and exposed at atmospheric pressure for predetermined times, t_r (2 hr $< t_r <$ 15 hr) and selected temperatures, T_r (570 K $< T_r <$ 670 K) to flowing Cl_2 in N_2, Cl_2 + NO in N_2, and Cl_2 + CO in N_2. When metal losses were expected, a silica wool plug was placed in the exit of the reactor for deposition of the volatile compound. The exposure was terminated by flushing with N_2 or He and the catalyst was allowed to cool to ambient. The catalyst samples were subsequently examined by XRD, TEM, and TPR. The methods and procedures have been described earlier (*2, 4*).

RESULTS

Conversion data for the different catalysts at selected values of temperatures and exposure times in 10% Cl_2 in N_2, 5% Cl_2 + 5% NO in N_2, and 8% Cl_2 + 2% CO in N_2 are given in Table 1, which also lists the TPR peak-maximum temperatures. The conversion was calculated from the amounts of H_2 consumed during TPR, assuming a stoichiometry of 2.0 molecules H_2 for each Pt atom and 1.5 molecules H_2 for each Ir atom.

TABLE 1

Results of the Reaction of Chlorine with the Catalysts

Catalyst	Treatment			% Metal converted[a]	TPR peak maximum (K)
	Gas composition (vol%)	Temp., T_r (K)	Time t_r (hr)		
A	10% Cl_2 90% N_2	570	3.0	100	500
A1	10% Cl_2 90% N_2	670	3.0	65[b]	400,500
B	10% Cl_2 90% N_2	670	2.0	58[c]	350,500
C	10% Cl_2 90% N_2	670	2.0	65[d]	500
C	10% Cl_2 90% N_2	670	4.0	80[d]	500
C	10% Cl_2 90% N_2	670	6.0	95[e]	500
D	10% Cl_2 90% N_2	670	15.0	90[f]	480
B	5% Cl_2 5% NO 90% N_2	670	2.0	100[e]	500
B	8% Cl_2 2% CO 90% N_2	670	2.0	100[g]	

[a] Calculated from TPR assuming Pt(4+) and Ir(3+) or from peak areas under XRD peaks.
[b] 100% of Pt and 30% of Ir converted.
[c] 100% of Pt and 12% of Ir converted. Large and small particles present after TPR.
[d] Both large (unreacted) and very small metal particles present on alumina after TPR.
[e] Mainly very small particles after reduction.
[f] Only about 55% metal remained on the catalyst, 45% was carried over and deposited on the cooler walls of the reactor.
[g] Extensive metal losses from the catalyst.

(1) Catalyst Structure after Reaction with Chlorine

Bimetallic catalysts. The particles of Catalyst A ($\bar{d} < 2$ nm) were converted completely to halides after reaction with 10% Cl_2 in N_2 at T_r = 570 K for t_r = 3 hr. For Catalyst C ($\bar{d}$ = 100 nm), complete conversion was achieved at T_r = 670 K, t_r = 6 hr. TEM images of the residual metal particles from catalyst C after reaction with 10% Cl_2 in N_2, T_r = 670 K, t_r = 2, 4 and 6 hr, respectively, are shown in Fig. 2. Figure 3 shows XRD stepscans across the 2θ region of the

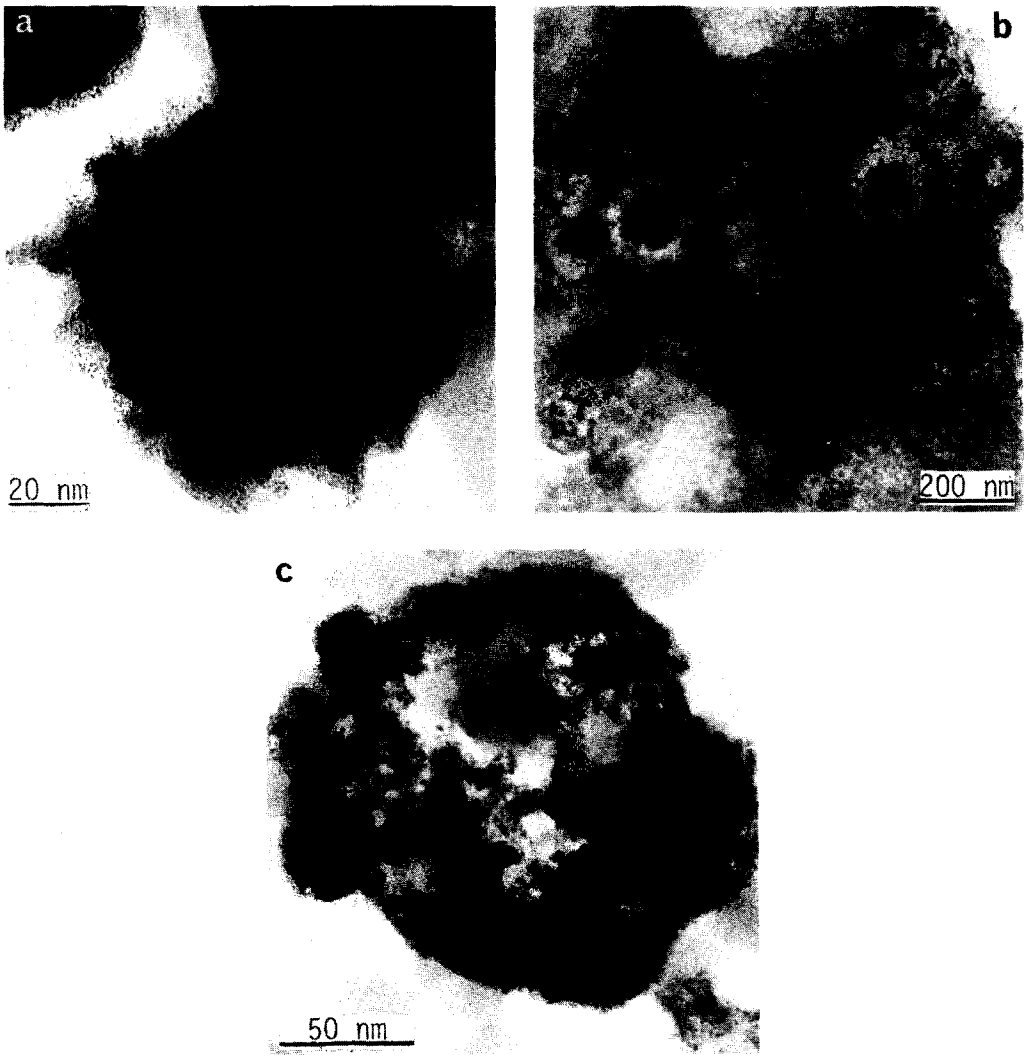

FIG. 2. Electron micrographs of Catalyst C after reaction in 10% Cl_2 in N_2 at T_r = 670 K for: (a) t_r = 2 hr, (b) t_r = 4 hr, and (c) t_r = 6 hr.

metal 111 peaks both before and after treatment. As the reaction proceeded, the intensity of the alloy peak decreased uniformly, with peak maximum remaining at 2θ = 61.3°. TEM images taken after treatment at T_r = 670 K for 2 hr showed thin chloride layers around the metal particles (Fig. 2a). These layers did not build up on further treatment although metal was still converted, as illustrated by the lighter areas around the residual metal in Fig. 2b. After t_r = 6 hr, most of the metal had been converted, but occasionally particle fragments honeycombed with holes and with jagged edges were seen (Fig. 2c). The SiO_2-supported Catalyst D behaved in a similar manner to that described for Catalyst C when treated with 10% Cl_2 in N_2 for various times; e.g., after t_r = 15 hr, a barely detectable metal 111 peak (see Fig. 11) indicated almost complete conversion of the metals to halides. However, in contrast to the alumina-supported Catalysts A and C, where no metal losses were observed, 45% of the metal was lost from the SiO_2 when Catalyst D was treated in 10% Cl_2 in N_2, T_r = 670 K, t_r = 15 hr.

No crystalline chloride could be detected

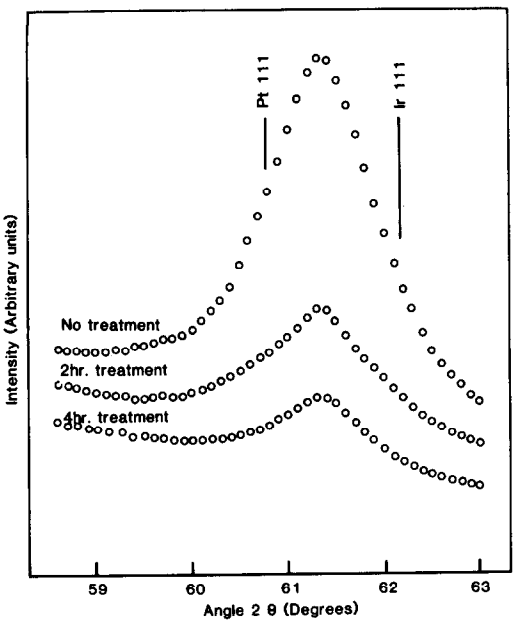

FIG. 3. XRD stepscans across the 2θ region of the 111 peaks for Pt and Ir in Catalyst C before and after treatment with 10% Cl_2 in N_2 for t_r = 2–4 hr. Radiation: CrKα (V-filtered).

with XRD after chlorine treatment of silica- or γ-alumina-supported bimetallic catalysts. However, lattice imaging of product layers formed around partially converted Pt–Ir particles in Catalyst C revealed an interlayer spacing of 0.62 nm (Fig. 4) between $PtCl_2$ (0.69 nm) and $IrCl_3$ (0.57 nm). The material collected on a silica plug in the reactor outlet tube when Catalyst D was treated with Cl_2 was also noncrystalline. After sequential oxidation and reduction of this substance, an XRD stepscan across the metal 111 2θ region (Fig. 5) indicated the presence of both platinum and iridium.

Mixed-metal catalysts. In Catalyst B and Catalyst A1, each of which contained separate Pt and Ir particles, treatment with 10% Cl_2 in N_2 resulted in the preferential conversion of platinum. For example, a comparison of the XRD traces in Figs. 6a and c shows that at T_r = 670 K, t_r = 2 hr, the Pt 111 peak in Catalyst B had disappeared, whereas the Ir 111 peak was only slightly reduced. A scan across the region of the strongest peaks of $PtCl_2$ and $IrCl_3$ showed that no significant amounts of crystalline chlorides were produced. Similarly for Catalyst A1, which contained both large iridium and small platinum particles, the XRD traces in Fig. 7 show that after treatment at T_r = 670 K, t_r = 3 hr, the Ir 111 peak is still about 85% of that observed before treatment. Again no $PtCl_2$ or $IrCl_3$ peaks are apparent.

Addition of NO to the treatment gas brought about conversion of both metals. Examination of XRD traces of Catalyst B after treatment with 5% Cl_2 + 5% NO in N_2, T_r = 670 K, t_r = 2 hr, showed that both metal 111 peaks had disappeared, but no platinum or iridium chloride peaks were seen. In CO–Cl_2 mixtures (8% Cl_2 and 2% CO) both metals were converted at T_r = 670 K after t_r = 2 hr, but substantial amounts of metal were lost from the catalyst.

(2) Temperature-Programmed Reduction (TPR)

TPR profiles of catalyst A are shown in Fig. 8. TPR of the catalyst precursor gave a broad profile with a maximum at 450 K, and the reduction stoichiometry, calculated from the hydrogen consumption and the

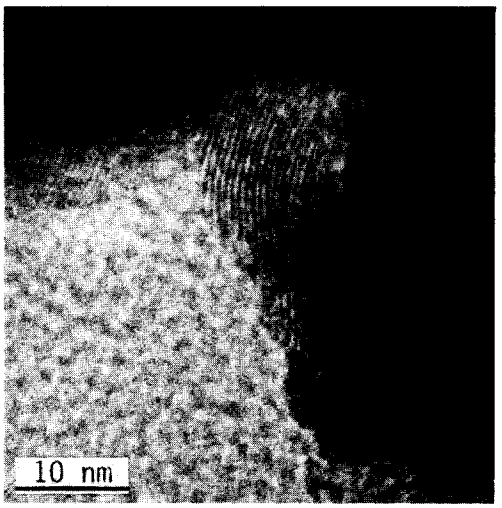

FIG. 4. Electron micrograph showing the lattice image of the compound formed around Pt–Ir particles in Catalyst C by treatment in 10% Cl_2 in N_2 at T_r = 670 K and t_r = 2 hr. The magnification was calibrated against the lattice spacing of anatase (0.35 nm) used as the internal standard. The measured spacing is 0.62 nm.

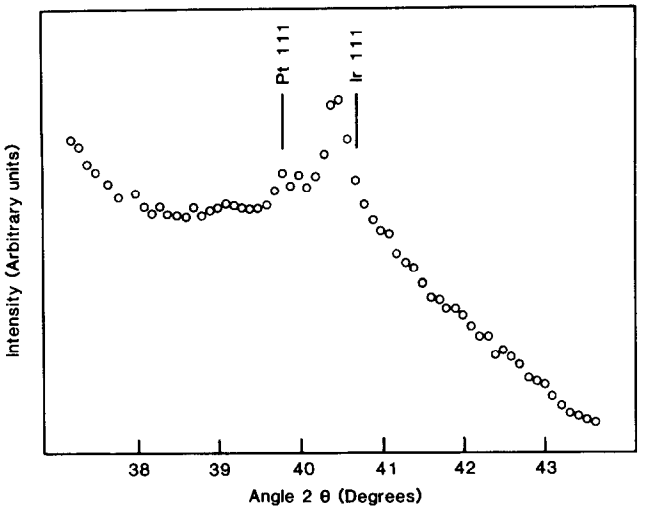

FIG. 5. XRD stepscan across the 2θ region of the 111 peaks of Pt and Ir for particles formed by oxidation (T = 770 K) and reduction from the volatile compound which sublimes out of Catalyst D during treatment in 10% Cl_2 in N_2 at T_r = 670 K and t_r = 15 hr. Radiation: CuKα (Ni-filtered).

metal content of the catalyst, was found to have a value between 2.0 and 2.1. Treatment of the reduced catalyst in 10% Cl_2 in N_2, T_r = 570 K, t_r = 3 hr, formed a product which gave a somewhat narrower TPR profile with a maximum at 500 K. Since increasing t_r to 5 hr did not affect the TPR result, 100% conversion of metal to halide was obtained after 3 hr. The stoichiometry

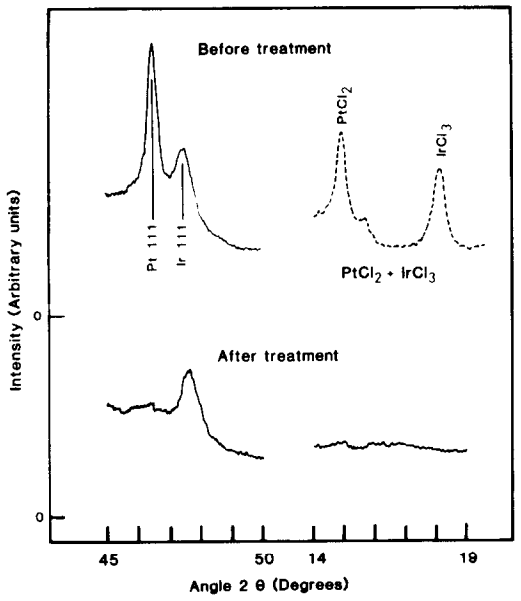

FIG. 6. XRD profiles of the Pt 111 and Ir 111 peaks of Catalyst B before and after treatment (10% Cl_2 in N_2, T_r = 670 K, t_r = 2 hr). A scan across the most intense $PtCl_2$ and $IrCl_3$ peaks is shown for Catalyst B after treatment together with a reference trace of a mixture of $PtCl_2$ and $IrCl_3$ on Al_2O_3. Radiation: CuKα (Ni-filtered).

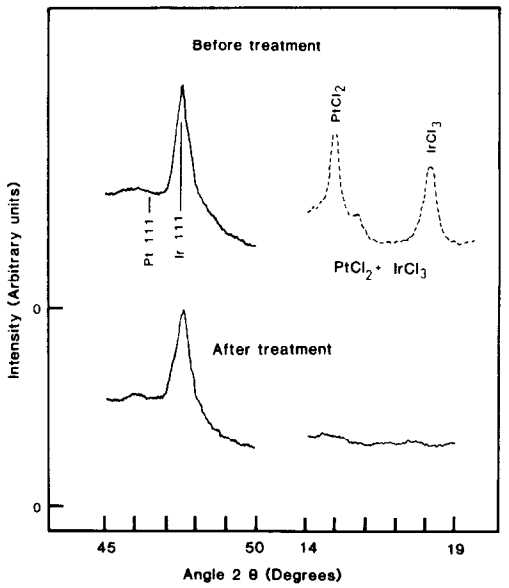

FIG. 7. XRD traces across the region of the 111 peaks of Pt and Ir and the most intense $PtCl_2$ and $IrCl_3$ reflections in Catalyst Al before and after treatment (10% Cl_2 in N_2, T_r = 670 K, t_r = 3 hr). A reference trace of a mixture of $PtCl_2$ + $IrCl_3$ on Al_2O_3 is also shown. Radiation: CuKα (Ni-filtered).

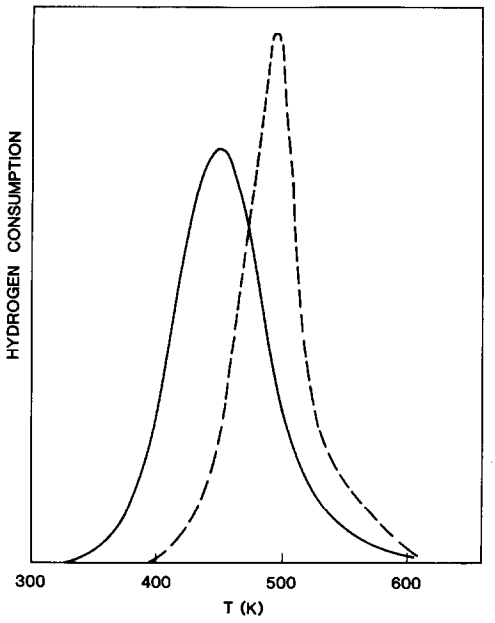

FIG. 8. TPR profiles of Catalyst A: catalyst precursor (—); after treatment with 10% Cl_2 in N_2 at T_r = 670 K and t_r = 3 hr (---). Sample weight, 0.1 g; temperature increase, 10 K min^{-1}.

of reduction of the chloride was 1.8, indicating an oxidation state of 4+ for platinum and 3+ for iridium.

TPR traces of Catalyst B are given in Fig. 9. In this case the catalyst precursor gave rise to peaks at 320 and 450 K. From comparisons with TPR of $PtCl_2/\gamma$-Al_2O_3 and $IrCl_3/\gamma$-Al_2O_3, and from XRD traces of partially reduced catalysts, the peak at 320 K was attributed to reduction of $PtCl_2$ and that at 450 K to reduction of $IrCl_3$. After treatment of Catalyst B in 10% Cl_2 in N_2, T_r = 670 K, t_r = 2 hr, TPR showed a small peak at 350 K and a larger one at 500 K. The peak of 350 K can be attributed either to the presence of small amounts of $PtCl_2$ or to thin $IrCl_3$ envelopes surrounding Ir particles. Such layers have been found previously to reduce at significant lower temperatures compared to bulk $IrCl_3$ (*5*). Addition of NO to the treatment gas resulted in complete conversion of both metals, so that after reaction with 5% Cl_2 + 5% NO in N_2, T_r = 670 K, t_r = 2 hr, only a single maximum at 500 K was seen.

(3) Catalyst Structure after Chlorine Treatment and Reduction

Bimetallic catalysts. Very small particles evenly distributed over the alumina support were present after reduction of Catalyst A which had been completely reacted with chlorine. EXAFS (*6*) gave a metal–metal nearest-neighbor distance identical to that obtained from the untreated catalyst (0.2742 nm). After reaction of the large alloy particles (>100 nm) in Catalyst C with 10% Cl_2 in N_2 at T_r = 670 K for t_r = 2 hr followed by TPR, very small (<2 nm) metal particles and residual unreacted alloy particles were observed on the alumina substrate (Fig. 10a). For t_r = 6 hr, only small metal particles were detected (Fig. 10b), except for the occasional only partially converted particle fragment (Fig. 2c). In Catalyst D, both small and large particles are present after chlorine treatment

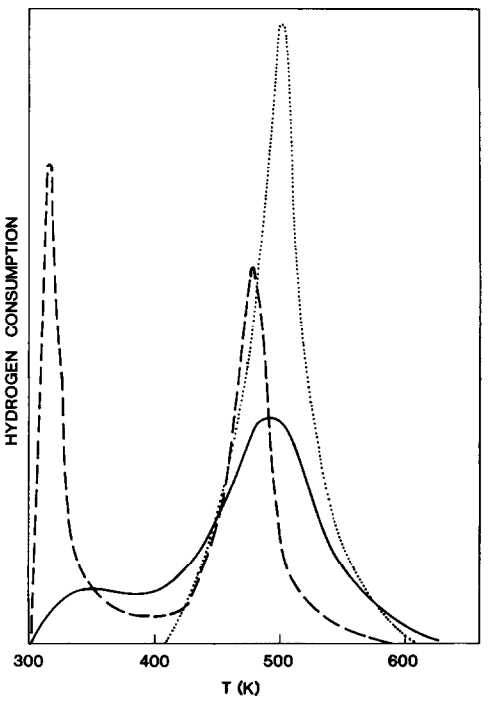

FIG. 9. TPR profiles of Catalyst B: catalyst precursor (---); after treatment at T_r = 670 K for t_r = 2 hr with 10% Cl_2 in N_2 (—); and 5% Cl_2–5% NO in N_2 (...). Sample weight, 0.1 g; temperature increase, 10 K min^{-1}.

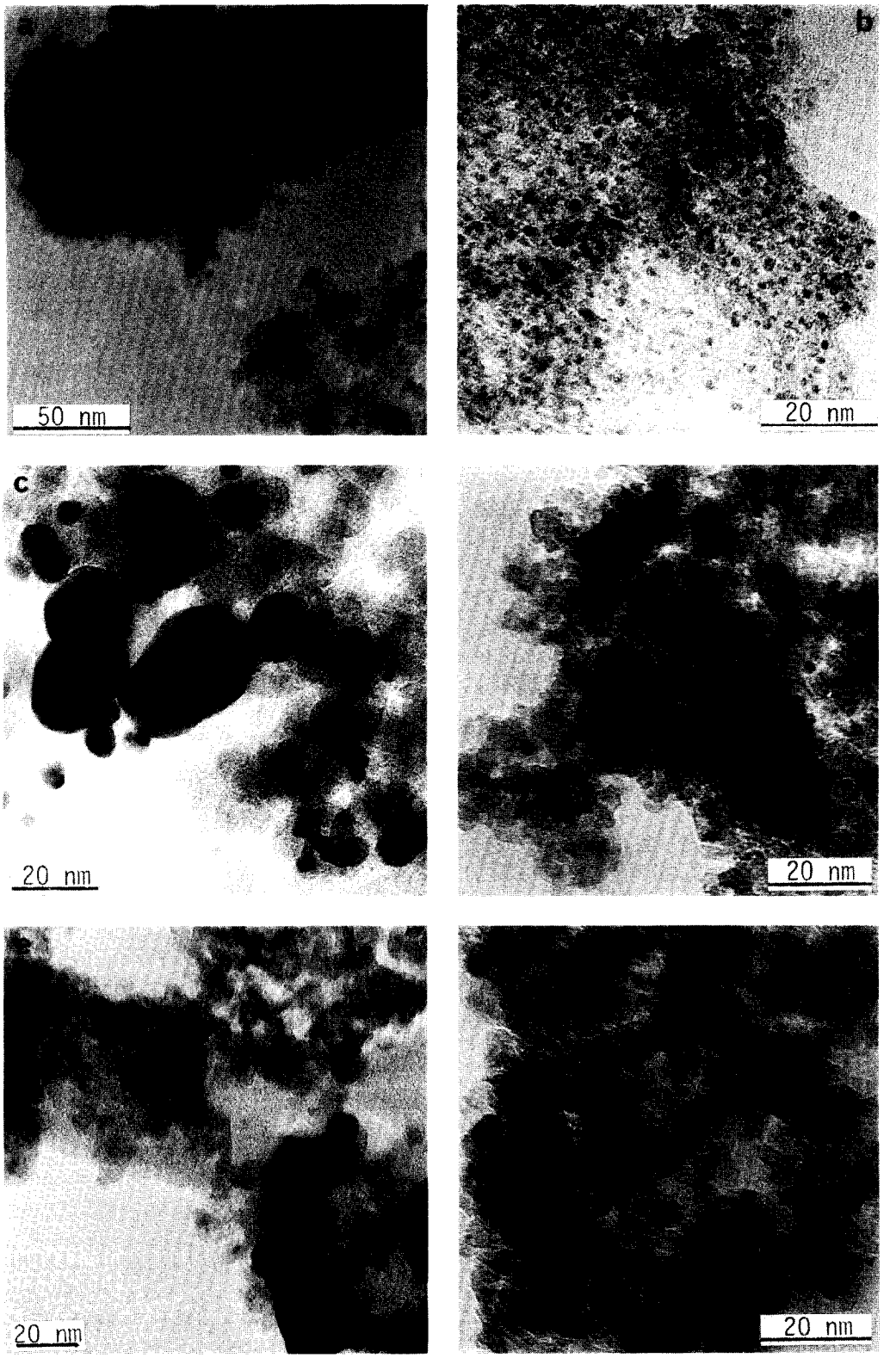

FIG. 10. Electron micrographs of catalysts after indicated treatment at T_r = 670 K followed by TPR. Catalyst C: 10% Cl_2 in N_2 for (a) t_r = 2 hr and (b) t_r = 6 hr; Catalyst D: 10% Cl_2 in N_2 for (c, d) t_r = 15 hr; Catalyst B: 10% Cl_2 in N_2 for (e) t_r = 2 hr, and (f) 5% Cl_2–5% NO in N_2 for t_r = 2 hr.

and TPR (Figs. 10c and d). XRD across the metal 2θ region showed that the peak position was the same as that of the catalyst before treatment (Fig. 11).

Mixed-metal catalysts. After treatment of Catalyst B in 10% Cl_2 in N_2, T_r = 670 K, t_r = 2 hr, followed by TPR, large (>50 nm) and very small (<2 nm) particles were seen (Fig. 10e). The XRD trace of this catalyst (Fig. 6) exhibited only an Ir 111 peak indicating that the small particles are Pt and the large ones Ir. After treatment with 5% Cl_2 + 5% NO in N_2, T_r = 670 K, t_r = 2 hr, followed by TPR, only small particles were detected with TEM (Fig. 10f), and no peaks could be seen in XRD traces. In contrast Cl_2/NO ratios >2 were required in order to achieve substantial redispersion of pure iridium catalysts, while at ratios lower than that, large sheets of $IrCl_3$ were formed (*5*). We believe that this difference is caused by the formation of surface-bound platinum-chloride species in mixed-metal catalysts which act as anchoring sites for the iridium-chloride phase.

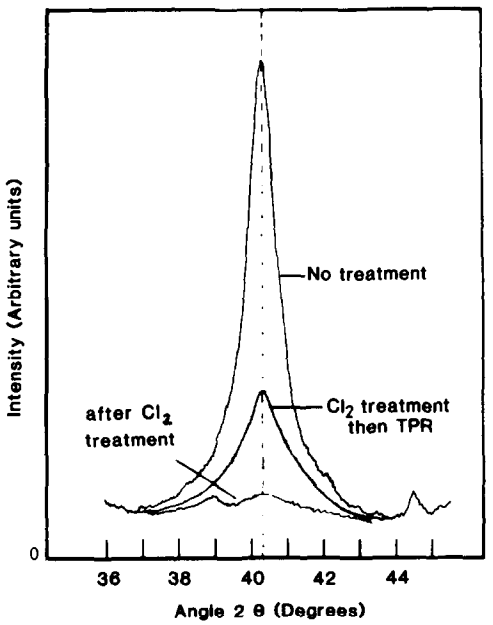

FIG. 11. XRD profiles across the 2θ region of Pt 111 (39.80°) and Ir 111 (40.65°) for Catalyst D before and after treatment in 10% Cl_2 in N_2, T_r = 670 K, t_r = 15 hr. Radiation: CuKα (Ni-filtered).

DISCUSSION

(1) Reaction of Pt–Ir Catalysts with Chlorine

Detailed studies of the reaction of supported platinum (*4*) and supported iridium (*5*) with chlorine revealed the following information:

(i) Pt supported on either SiO_2 or γ-Al_2O_3 reacted readily with chlorine to form β-$PtCl_2$, and complete conversion of metal particles as large as 100 nm could be achieved at T_r = 470 K with reaction times of several hours.

(ii) Ir proved significantly more resistant to attack by chlorine, and temperatures of >700 K were necessary to achieve conversion of large Ir particles to α-$IrCl_3$.

(iii) On SiO_2, β-$PtCl_2$ agglomerated to large crystals, and at temperatures >550 K, sublimed out of the catalyst bed. On γ-Al_2O_3, however, β-$PtCl_2$ was readsorbed and reacted with further chlorine to form stable surface-anchored chloride complexes of Pt(IV). Reduction of these complexes resulted in small metal particles (<2 nm), while crystalline $PtCl_2$ transformed into large Pt agglomerates.

(iv) The low volatility of α-$IrCl_3$ prevented vapor-phase transport and redistribution on the substrate surface below 750 K and the compound built up layers around iridium particles. In order to achieve redistribution of Ir, volatilizing agents such as CO or NO had to be added to the treatment gas.

On the basis of these results it was expected that the reaction of chlorine with Pt–Ir catalysts would result in preferential conversion of platinum. This could have been confirmed by examination of the XRD 111 alloy peak position after various extents of reaction. Preferential conversion of one component in an alloy system would cause a shift of the XRD peak toward the position of the second component as observed, for example, during the treatment of Pt–Ir in O_2-containing atmospheres, where iridium is preferentially oxidized and the XRD 111

peak is shifted toward the Pt 111 peak position (*2*). In the case of Catalysts A1 and B, both of which contain a mixture of platinum and iridium particles, preferential reaction of Pt is indeed occurring. For example, after treatment of Catalyst B with 10% Cl_2 in N_2, T_r = 670 K, t_r = 2 hr, the XRD trace shows no remaining Pt 111 peak, while the Ir 111 peak is largely unaffected (Fig. 6). Extensive conversion of both metals occurred in 5% Cl_2 + 5% NO in N_2 and in 8% Cl_2 + 2% CO in N_2. This is in agreement with the earlier finding that addition of NO or CO to the treatment gas accelerates the reaction of iridium with chlorine (*5*).

In contrast, on bimetallic Pt–Ir catalysts the XRD alloy 111 peak loses intensity and finally disappears completely as the reaction proceeds, but at no time does its position change, suggesting a simultaneous conversion of both metals to chlorides. The rate of chlorination of Pt–Ir is somewhat slower than that observed previously for platinum (*4*) but considerably faster than that found for iridium (*5*). For example, Pt–Ir particles as large as 100 nm are totally converted to halides at T_r = 670 K, t_r = 6 hr, while under similar conditions, large iridium particles are attacked by chlorine only very slowly. The product formed from alloy particles, either on SiO_2 or γ-Al_2O_3, could not be identified by XRD. Chloride layers of dimensions similar to those seen around iridium particles after chlorine treatment were not generally observed around Pt–Ir particles. However, product layers could be seen enveloping partially converted Pt–Ir particles (Fig. 2a). Lattice imaging of this layer (Fig. 4) gave an interlayer spacing of 0.62 nm intermediate between those reported for β-$PtCl_2$ (0.69 nm) or α-$IrCl_3$ (0.57 nm).

The volatility of this compound is intermediate between that observed for β-$PtCl_2$, highly volatile, and α-$IrCl_3$, characterized by low volatility. To illustrate this point, 45% of Pt–Ir sublimed out of Catalyst D after treatment with 10% Cl_2 in N_2 at T_r = 670 K for t_r = 15 hr. By comparison it was previously observed that nearly 90% of the platinum was lost from a Pt on SiO_2 catalyst at T_r = 670 K for t_r = 2 hr (*4*). Ir was not transported from Ir on SiO_2 catalysts at temperatures <750 K (*5*). An analysis of the material sublimed from Catalyst D and trapped in the colder exit of the reactor gave a ratio of Pt to Ir close to the one of the original alloy. This suggests simultaneous transport of both metals. We propose the following possibilities for simultaneous vapor-phase transport of Pt and Ir by chlorine:

(i) formation of volatile adduct compounds of composition intermediate between $PtCl_2$ and $IrCl_3$ or

(ii) incorporation of iridium into the highly volatile, hexameric Pt_6Cl_{12} molecule.

ad (i) Schäfer *et al.* (*8*) studied chemical vapor-phase transport reactions of noble metal halides in the presence of aluminum and iron halides, and reported that the addition of the latter compounds caused a marked increase in the volatility of the noble metal halides. Furthermore, it accelerated the chlorination reaction by removing inhibiting halide layers from the surface of the metal particles. A large variety of halides was reported to form volatile complexes with $AlCl_3$ (*8, 9*), generally of the type $PtAl_2Cl_8$ ($PtCl_2 \cdot Al_2Cl_6$). Such adduct complexes are commonly unstable in the solid phase and decompose on deposition into compounds such as $PtCl_2$ and $AlCl_3$. If adducts between $PtCl_2$ and $IrCl_3$ did exist, they had to be stable both in the gas and solid phases, since neither crystalline $PtCl_2$ nor $IrCl_3$ was found in the deposit from Pt–Ir catalysts. Brodersen *et al.* (*10*) reported mixed-crystal formation between $RuCl_3$ and $IrCl_3$, but did not give data on the structure and properties of the compound.

ad (ii) The hexameric molecule Pt_6Cl_{12} consists of an octahedrally arranged core of Pt_6 with a bridging chloride atom above each of the 12 edges of the octahedron (*11*). Progressive substitution of iridium for platinum atoms would be expected to distort this structure, in view of the different

metal–chlorine bond length. If such a product were formed, this could account for the lack of crystallinity of the vapor-phase deposit in the exit tube of the reactor after passing 10% Cl_2 in N_2 over Catalyst D at T_r = 670 K.

To our knowledge mixed halides containing both Pt and Ir have not been reported in the literature before. However, their existence cannot be dismissed, particularly considering the limited published data on iridium-halide chemistry.

(2) Redispersion of Pt–Ir Catalysts

The present results show that the effectiveness of the redispersion of agglomerated metal in Pt–Ir catalysts by chlorine treatment depends on two factors:

(i) the type of support material and

(ii) whether bimetallic particles or a mixture of separate Pt and Ir particles are present in the catalyst.

Chlorine treatment followed by reduction of the alumina-supported bimetallic Catalyst C resulted in the formation of very small metal particles, while similar treatment of the silica-supported Catalyst D resulted in larger metallic particles. Similar behavior was observed for the redispersion of Pt on both silica and alumina (*4*). In this case γ-Al_2O_3 provided strong anchoring sites for the anionic chloride-product complexes of Pt(IV), whereas SiO_2 surfaces which exhibit anionic exchange properties in extremely acid media only, but otherwise are cation absorbers, provide no such anchoring sites. Small metal particles resulting from the redispersion treatment of alloy catalysts are bimetallic. This is supported by (i) the nearest-neighbor distance of 0.2742 nm between metal atoms in particles present in the reduced chlorine-treated Catalyst A was intermediate between Pt–Pt (0.2775 nm) and Ir–Ir (0.2714 nm); (ii) the position of the XRD peak obtained from the larger particles present in Catalyst D after redispersion treatment followed by reduction was typical for a Pt–Ir alloy phase (*vide* Fig. 11); and (iii) our finding that the volatile halide compound responsible for the redispersion contained Pt and Ir.

When separate Pt and Ir particles, and in particular large iridium agglomerates (as would be the case after coke burnoff in oxidizing atmospheres at temperatures >700 K), are present, simply treating the catalyst with chlorine cannot achieve redispersion of both metals. For example, our results for Catalysts A1 and B show that in such a system Pt is preferentially redispersed while Ir stays in the form of large separate aggregates. Chlorine by itself was found to be ineffective for the redispersion of Ir, due to the low volatility of the chloride-product phase below 750 K and/or its limited interaction with the substrate surface. However, mixtures of CO with Cl_2 (in N_2) in ratios <0.3 and of NO and Cl_2 (in N_2) in ratios <0.5 proved substantially more useful in dispersing agglomerated Ir (*5*). A redispersion process for Pt–Ir catalysts utilizing a mixture of CO and Cl_2 proved to be difficult to control, due to the high volatility of platinum carbonylchlorides (*12*). On the other hand, additions of NO to the chlorine-containing treatment gas gave adequate redispersion of both metals on the γ-alumina surface without metal losses, and after reduction metal particles <2 nm in size were found to predominate. The composition of these particles has not been determined, and the possibility that they were small separate particles of Pt and Ir cannot be ignored. However, Garten and Sinfelt (*13*) reported the preparation of Pt–Ir bimetallic clusters by coimpregnation as well as sequential impregnation methods, implying that the metal or metal compound first deposited on the substrate surface provides favorable anchorange sites for the second metal compound. Thus, we are confident that when catalysts comprising large separate particles of platinum and iridium are treated with mixtures of NO and Cl_2, highly dispersed bimetallic Pt–Ir catalysts result by deposition of the formed iridium compound in close proximity to the more read-

ily formed platinum-chloride complex bound to the γ-alumina substrate.

Recently, Fung *et al.* and Landolt *et al.* (*14*) have claimed that phase-separated Pt–Ir catalysts can be redispersed with Cl_2, Cl_2–O_2, Cl_2–H_2O, and HCl–O_2 if (i) the redispersion step is carried out at temperatures $\geq$770 K and (ii) the catalyst is *highly chlorinated prior* to the redispersion step by pretreatment with HCl in the absence of oxygen. A comparison of their claims with our study on the redispersion of Ir (*5*) leads to the conclusions that the highly chlorinated support surface created by HCl pretreatment interacts strongly with the metal halides formed in the redispersion step. Without the HCl pretreatment the interaction with the surface is weak and the metal halides agglomerate to large crystals.

CONCLUSIONS

(1) Alumina-supported bimetallic Pt–Ir catalysts are readily redispersed by treatment in a chlorine-containing reaction gas. The volatile species responsible for the redispersion of the metals on the support surface is a mixed chloride compound of platinum and iridium. It is either of the adduct type, as formed between $PtCl_2$ and $AlCl_3$ (i.e., $PtAl_2Cl_8$), or is more likely a hexameric molecule like Pt_6Cl_{12} with some platinum atoms exchanged for iridium. Evidence suggests that the small metal particles observed after reduction of the chlorine-treated catalysts have the same composition as the large alloy particles present before the redispersion treatment.

(2) After chlorine treatment of catalysts consisting of mixtures of separate Pt and Ir particles, only platinum is readily redispersed, while iridium agglomerates remain largely unchanged. Therefore, it is important to carry out coke burnoff at low temperatures in order to prevent separation of the two metals, although this may not always be possible.

(3) Redispersion of phase-separated Pt–Ir catalysts with mixtures of CO and Cl_2 is difficult to control because the formed platinum carbonylchloride species are extremely volatile.

(4) Mixtures of NO and Cl_2 are suitable for the redispersion of both Pt and Ir. Although the composition of the resulting small metal particles has not been determined, it is likely that they are bimetallic clusters.

REFERENCES

1. Sinfelt, J. H., U.S. Patent 3,953,368 (1976).
2. Foger, K., and Jaeger, H., *J. Catal.* **70,** 53 (1981).
3. Sittig, M., *in* "Handbook of Catalyst Manufacture," pp. 441–444. Noyes Data Corp., Park Ridge, N.J., 1978.
4. Foger, K., and Jaeger, H., *J. Catal.* **92,** 64 (1985).
5. Foger, K., Hay, D., and Jaeger, H., *J. Catal.* **95,** 154 (1985).
6. Foger, K., unpublished EXAFS data taken at the Stanford Synchrotron Laboratory.
7. Sinfelt, J. H., Via, G. H., and Lytle, F. W., *J. Chem. Phys.* **76,** 2779 (1982).
8. Schäfer, H., Wiese, U., Brendel, C., and Nowitzki, J., *J. Less-Common Met.* **76,** 63 (1980).
9. Schäfer, H., and Florke, U., *Z. Anorg. Allg. Chem.* **479,** 84 (1981).
10. Brodersen, K., Moers, F., and Schnering, H. G., *Naturwissenschaften* **52,** 205 (1965).
11. Brodersen, K., Thiele, G., and Schnering, H. G., *Z. Anorg. Allg. Chem.* **337,** 120 (1965).
12. Schäfer, H., and Wiese, U. J., *J. Less-Common Met.* **24,** 55 (1971).
13. Garten, R. L., and Sinfelt, J. H., *J. Catal.* **62,** 127 (1980).
14. (a) Fung, S. C., Rice, R. W., Weissman, W., Carter, J. L., and Kmak, W. S., EP 0.093,621 A1; U.S. 4,447,551; U.S. 4,444,895; U.S. 4,444,896; U.S. 4,444,897; (b) Landolt, G. R., McHale, W. D., and Schoenagel, H. J., GB 2,091,577A.